Semnan University

Innovations in Materials: Current and Future

Journal homepage: https://imcf.semnan.ac.ir

ISSN: 3115-9990

Research Article

Temperature and Concentration Effects on the Adsorption of Phenol, Formaldehyde, and Water on X70 Steel: A Molecular Dynamics Study

Hadi Eivazi Bagheri[a *], *Seyyed Salman Seyyed Afghahi*[a], *Ali Asghar Ebrahimi Valmoozi*[a]

Amir Hosein Bakhshandeh[b]

[a] *Faculty of Materials Science and Nanotechnology, Imam Hossein University, Tehran, Iran*

[b] *Department of Chemistry, Kharazmi University, Tehran, Iran*

ARTICLE INFO

Article history:

Received: 2025-07-31

Revised: 2025-09-29

Accepted: 2025-09-30

Keywords:

Molecular Dynamics Simulation (MD)

Surface Adsorption

X70 steel

RDF

ABSTRACT

This study employs molecular dynamics (MD) simulations to investigate the influence of temperature and molecular quantity on the adsorption of phenol, formaldehyde, and water on API 5L X70 steel. The results demonstrate that elevated temperatures reduce adsorption for all substances, as increased kinetic energy promotes desorption, evidenced by lower peaks in radial distribution function (RDF) curves. Conversely, increasing the molecular quantity generally enhances the density within the first adsorbed layer, indicated by higher RDF peaks, though the magnitude of this effect is substance and temperature-dependent. Phenol exhibited stronger individual adsorption affinity than water or formaldehyde. In competitive adsorption from mixtures, phenol and formaldehyde showed aff significant rivalry for surface sites, with the preferential adsorption dictated by the interplay between temperature and concentration. These findings elucidate the molecular interactions governing the behavior of these organic compounds at the steel-fluid interface, providing critical insights for predicting material performance in high-temperature corrosive environments, such as autoclaves and furnaces used for composite curing.

1. Introduction

Corrosion of steels remains a major industrial challenge, causing significant economic losses, structural failures, environmental hazards, and even threats to human safety [1–3]. High-strength low-alloy (HSLA) steels, such as API X70, are widely used in demanding applications, including autoclave shells, due to their favorable combination of mechanical strength and durability [4]. These steels are typically strengthened through the addition of minor alloying elements such as molybdenum, niobium, titanium, and vanadium, which enhance mechanical properties via grain refinement, solid-solution strengthening, and precipitation hardening [5]. Despite these improvements, HSLA steels remain susceptible to degradation under aggressive environmental conditions, highlighting the need for effective corrosion prevention strategies.

*** Corresponding author.**
E-mail address: *hadi-bagheri@ihu.ac.ir*

Cite this article as:
Eivazi Bagheri, H., Seyyed Afghahi, S. S., Ebrahimi Valmoozi, A. A., & Bakhshandeh, A. H., 2026. Molecular dynamics simulation of the effect of phenol, formaldehyde and water on the API 5L Grade X70 steel surface. Innovations in Materials: Current and Future, 1(1), pp.3–11.
https://doi.org/ …

Extensive experimental studies have provided valuable insights into corrosion phenomena; however, they often cannot resolve atomic-scale interactions and are both time- and resource-intensive. In particular, the adsorption of corrosive species, such as water molecules or aggressive ions, remains poorly understood at the atomic level. These knowledge gaps emphasize the necessity of computational approaches capable of complementing experimental observations.

Molecular dynamics (MD) simulation is a well-established computational technique that models the behavior of atoms and molecules based on Newtonian mechanics and interatomic potentials[6].

In composite manufacturing—particularly with phenolic resins—the presence of formaldehyde and water result from chemical reactions occurring during curing. Phenolic resins are a class of thermosetting polymers produced by reacting phenol with formaldehyde in the presence of an acidic or basic catalyst. They are widely used across industries due to their thermal resistance, chemical stability, adequate mechanical strength, and relatively low cost. Phenol plays a key role in defining the resin's structure and properties, as its activated benzene ring is the primary reaction site for formaldehyde, while its hydroxyl group contributes to bond formation and the final resin characteristics. The phenol-to-formaldehyde ratio and reaction conditions determine the resin type and its properties. During curing, formaldehyde reacts with phenolic active groups to form methylene ($-CH_2-$) or ether ($-CH_2OCH_2-$) bridges between phenol molecules. Some formaldehyde may remain unreacted within the composite, and water is produced as a byproduct. The phenol–formaldehyde reaction is a condensation process in which water is eliminated, leading to crosslink formation and resin hardening[7].

By enabling the observation of atomic interactions over time, MD has been extensively employed in materials science, chemistry, and engineering to investigate processes that are challenging to capture experimentally. In the context of corrosion, MD simulations facilitate detailed examination of interactions between metal surfaces and corrosive media, including adsorption phenomena, inhibitor efficacy, and structural evolution at the metal–solution interface. MD offers atomic-scale resolution, predictive capability, and the potential to reduce reliance on costly experimental procedures.

In this work, MD simulations are employed to investigate the adsorption behavior of phenol, formaldehyde, and water molecules on the API X70 steel surface in corrosive media. The study aims to elucidate the fundamental atomic-scale mechanisms governing corrosion processes, thereby providing insights that may inform future investigations into protective strategies for HSLA steels.

Several studies have investigated the effects of various elements and conditions on X70 steel surfaces. Bej et al. [8] examined the early stages of corrosion formation on API X70 pipeline steel under an oxy-fuel atmosphere using a simulated gas mixture for 15 hours at 278 K and ambient pressure, observing localized pitting corrosion and predominantly amorphous corrosion products with some partial crystallinity. Ahmad et al. [9] investigated the inhibition of X70 steel corrosion in aerated 3 wt% NaCl solution using cerium(III) nitrate hexahydrate, employing polarization measurements, electrochemical impedance spectroscopy (EIS), and scanning electron microscopy (SEM). They found that increasing Ce(III) concentration enhanced protective efficiency, reaching an optimal value of 72%. Guillermo et al. [10] synthesized a new series of carbohydrate–xanthine derivatives and evaluated their inhibition performance toward API 5L X70 steel corrosion in 1 M HCl, achieving 90% inhibition efficiency at a dosage of 10 ppm, as revealed by EIS. Guo et al. [11] employed electrochemical techniques and weight-loss measurements to probe the inhibition mechanism of mango leaf extract on X70 steel corrosion in 1 M HCl, demonstrating enhanced inhibition at higher concentrations and lower temperatures. Xiang et al. [12] explored the effect of temperature on X70 steel corrosion in high-pressure $CO_2/SO_2/O_2/H_2O$ mixtures, showing that the corrosion rate increased with temperature up to 348 K and then declined; detected hydrogen in the outlet gas was attributed to cathodic hydrogen evolution. Vazquez et al. [13] assessed spirodioxynaphthalene preussomerin G—isolated from Pyrenochaetopsis sp. T1-41—as a corrosion inhibitor for API 5L X70 steel, demonstrating good inhibition under static conditions. Wei et al. [14] simulated electrochemical corrosion behavior in saline soil using a one-dimensional soil column apparatus, showing that capillary water ascent significantly affects X70 steel corrosion. Behlake et al. [15] sed MD simulations to examine epoxy systems modified with aminoamide agents for coating formation on iron-oxide surfaces, demonstrating that longer polymer chains enhance epoxy–oxide interactions.

2. Materials and Methods

The adsorption processes of phenol, formaldehyde, and water vapors were investigated using molecular dynamics (MD)

simulations using the LAMMPS software. Structural analyses, notably the radial distribution function (RDF), were employed to characterize the adsorptive behavior at the steel surface. Three system sizes—containing 150, 200, and 250 molecules—were each simulated at four temperature levels: 298, 373, 473, and 573 K.

2.1. Model Construction

To model the polycrystalline API 5L X70 steel, Atomsk was employed to generate its atomic configuration. Because surface adsorption was the primary focus and the steel substrate remained rigid, the simulation cell was defined as 1 Å thick with 50 Å × 50 Å lateral dimensions. The thickness of 1 Å was chosen intentionally to represent only the outermost atomic layer of the steel surface, since the objective of this work was to investigate surface–molecule interactions rather than bulk alloy properties. This approach significantly reduces the computational cost while still capturing the essential atomistic details of adsorption phenomena. To simplify the system, only the major alloying elements—97.8 mol % Fe, 1.5 mol % Mn, 0.5 mol % Si, and 0.2 mol % C—were included. Table 1 summarizes the detailed chemical composition, and Figure 1 presents the equilibrated atomic structure of the constructed X70 steel model.

Table 1. Chemical Composition Analysis of API 5L X70 Steel

Element	Composition (wt%)
Fe	97.701
C	0.064
Si	0.258
Mn	1.581
Cr	0.184
Ni	0.06

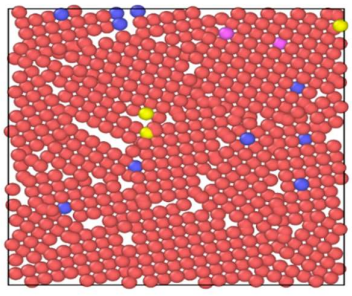

Fig. 1. Atomic structure of the API 5L X70 steel slab generated with Atomsk (1 Å thickness; 50Å × 50Å lateral dimensions ; Fe = red, Mn = blue, Si = yellow, C = purple).

The molecular structures of phenol, formaldehyde, and water were first built using GaussView. These structures were then replicated to system sizes of 150, 200, and 250 molecules each, using Packmol. Figure 2 illustrates the Packmol-generated simulation box containing 200 molecules of each species.

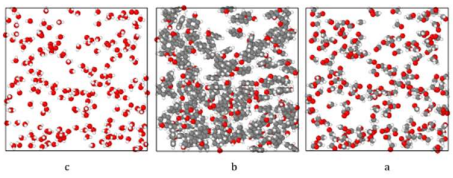

Fig. 2. Packmol-generated simulation boxes containing 200 molecules of each species: (a) formaldehyde, (b) phenol, and (c) water.

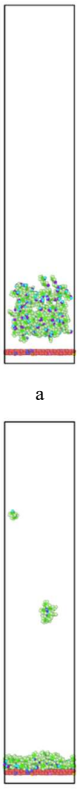

Fig. 3. Final simulation box for 150 phenol molecules on the API 5L X70 steel surface. a) first frame b) last frame

The final simulation systems—comprising phenol–steel, formaldehyde–steel, and water–steel interfaces were constructed in Materials Studio. The lateral dimensions of the simulation box were set to 50 Å × 50 Å, which are identical to those of the steel substrate. The substrate itself consisted of 609 atoms, including 594 Fe, 10 Mn, 2 C, and 3 Si atoms, thereby reproducing the chemical composition of API 5L X70 as reported in Table 1. The height of the simulation box was extended to 255 Å to provide sufficient space for

the movement of the adsorbed molecules. This configuration offers a representative atomic-scale model of the alloy while maintaining computational feasibility and accuracy for molecular dynamics simulations. The fully assembled system was then exported as a data file from Materials Studio. Figure 3 depicts the simulation box prepared for 150 phenol molecules interacting with an API 5L X70 steel surface.

2.2. Molecular Dynamics Simulations

A total of 38 simulation boxes were prepared, each with a minimum separation of 15 Å between the adsorbate molecules and the steel surface to ensure that the adsorption tendency could be evaluated relative to their initial positions. Periodic boundary conditions were applied along the x and y directions to mimic the infinite steel surface, while a non-periodic boundary was defined in the z direction to allow sufficient space for molecule adsorption and diffusion above the surface. The NVT ensemble was selected to maintain a constant number of particles, volume, and temperature, which is appropriate for studying adsorption processes at the metal–molecule interface where pressure fluctuations are not the primary concern. The Lennard–Jones (LJ) potential was used to describe van der Waals interactions between the steel surface and the adsorbed molecules, as it has been widely adopted for modeling physisorption phenomena. For water, the TIP3P model was employed because it is a well-established, computationally efficient, and extensively validated water model in molecular dynamics simulations. These assumptions and choices were made to ensure a balance between computational efficiency and physical accuracy in representing the corrosion and inhibition processes under study. All simulations were carried out in the NVT ensemble for 1 ns, corresponding to 1–2 million integration steps. Structural optimization during the simulations was performed using the conjugate-gradient minimization algorithm, and all MD settings were implemented in the LAMMPS package. The Lennard-Jones potential was used to describe the interactions between each adsorbate and the steel substrate[16, 17]. For water molecules, the TIP3P force field was employed[18].

Temperature control was achieved via the Nosé–Hoover thermostat, which is well suited to the NVT ensemble and automatically maintains the system at the target temperature. Steel atoms were held fixed, while phenol, formaldehyde, and water molecules were free to move within the simulation box. After the production runs, radial distribution functions (RDFs) between each adsorbate and the iron atoms in the steel were calculated using VMD, taking into account the high system density. Visualization of the final configurations was performed with OVITO.

In this study, only the radial distribution function (RDF) was calculated to examine the spatial distribution of adsorbate molecules near the steel surface. RDF provides useful insights into preferred distances and localization of molecules, although it cannot fully distinguish between permanent adsorption and transient encounters. Despite this limitation, RDF remains a widely used and informative metric for evaluating adsorption tendencies in molecular dynamics simulations.

3. Results and Discussion

In Fig. 4 a, b, and c, the radial distribution functions, g(r), for formaldehyde molecules in contact with API 5L X70 steel are presented for three concentrations (150, 200, and 250 molecules within the simulation cell) and four temperatures (298K, 373K, 473K, and 573K). Examining how g(r) varies with temperature and concentration provides key insights into formaldehyde's surface-adsorption behavior on X70 steel.

Across all three concentrations, increasing the temperature from 298K to 573K leads to a pronounced decrease in the height of the primary RDF peak at short distances from the surface. This reduction in peak intensity, which directly corresponds to the lower local density of first-layer adsorbed formaldehyde, and reflects an enhanced tendency for desorption as molecular thermal energy rises. At higher temperatures, the average kinetic energy surpasses the attractive van der Waals forces between formaldehyde and the steel, resulting in fewer molecules bound to the surface.

Under constant low-temperature conditions, (e.g, 298K, where adsorption is strongest), increasing the number of formaldehyde molecules from 150 to 200 and then to 250 strengthens the primary RDF peak. This enhancement indicates a higher local density of formaldehyde in the first adsorption layer, owing to the greater availability of molecules to occupy surface sites. In other words, at lower thermal energies, the steel surface can accommodate more formaldehyde in its first layer, and that layer becomes increasingly compact as concentration rises.

Comparing across all conditions reveals an interplay between temperature and concentration. The adsorption-reducing effect of temperature (manifested by a decrease in peak height) is present at every concentration and becomes most dominant at 573K, where overall adsorption is low and differences between concentrations shrink. Conversely, the

concentration-driven increase in peak height is most pronounced at 298K, where strong surface forces and intermolecular attractions prevail. This demonstrates that when thermal agitation is limited, raising the number of molecules plays a critical role in enhancing surface coverage and local density of formaldehyde on X70 steel.

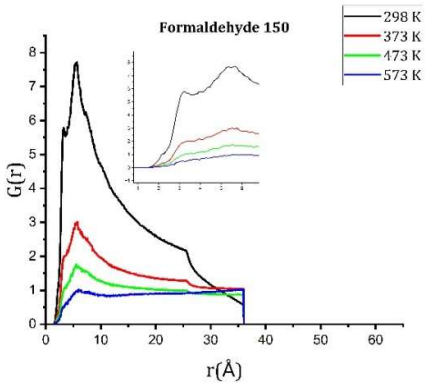

(a)

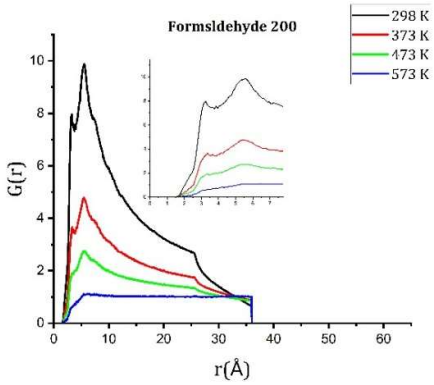

(b)

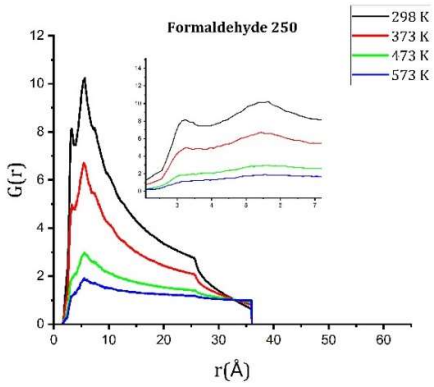

(c)

Fig. 4. Radial distribution functions for 150 (a), 200 (b), and 250 (c) formaldehyde molecules adsorbed on API 5L X70 steel at 298K, 373K, 473K, and 573K

In Fig. 5 a, b, and c, the radial distribution function (g(r)) for phenol molecules at three different concentrations (corresponding to 150, 200, and 250 molecules on the X70 steel surface) is shown at four temperatures: 298K, 373K, 473K, and 573K.

Analysis of the RDF data shows that increasing the temperature from 298K to 373K leads to a noticeable decrease in the height of the primary RDF peak. This peak represents the probability of finding phenol molecules at a specific distance from each other or from the steel surface and typically corresponds to the first adsorption layer near the surface. The reduction in peak height can be attributed to the increased thermal energy of the molecules, which enhances their vibrational motion and slightly disrupts the ordering within the adsorbed layer. Phenol molecules exhibit both an affinity for adsorption on the steel surface and the ability to form hydrogen bonds with each other, interactions that are more prominent at lower temperatures and contribute significantly to the structure of the surface layer.

As the temperature rises further to 473K and 573K, the kinetic energy of the molecules becomes high enough to overcome both the attractive interactions between phenol and the steel surface and the hydrogen bonding among phenol molecules. This results in a pronounced desorption of phenol from the surface and increased mobility in the region above it. In the RDF plots, this effect appears as a more substantial drop in the main peak height along with a broadening of the distribution at higher temperatures, indicating a marked decrease in molecular density and order near the surface.

The influence of phenol concentration is also clearly visible in the RDFs. As the number of molecules increases from 150 to 200 and then to 250, the main RDF peak becomes broader and its height decreases. This is likely due to full surface coverage followed by the formation of multilayers of phenol on top of the first adsorbed layer. Molecules in these additional layers can also engage in hydrogen bonding, but the arrangement becomes more disordered compared to a single, well-structured monolayer. This multilayer formation and intermolecular interaction contribute to increased structural disorder, especially at lower temperatures (298K and 373K), where thermal agitation is less dominant and molecular organization plays a more significant role. The disorder is reflected in the broadening of the RDF peak, which suggests a wider range of intermolecular distances due to less regular packing. Therefore, increasing the number of molecules not only alters the local density (as indicated by peak height) but also

affects the overall structural order, which is evident in the shape and width of the RDF peaks.

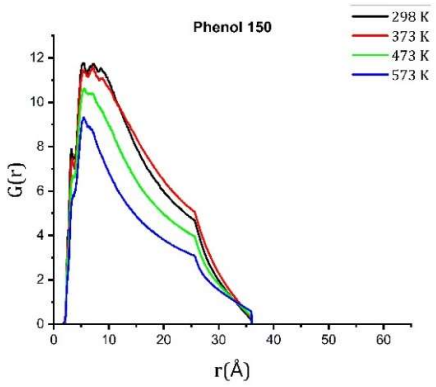

(a)

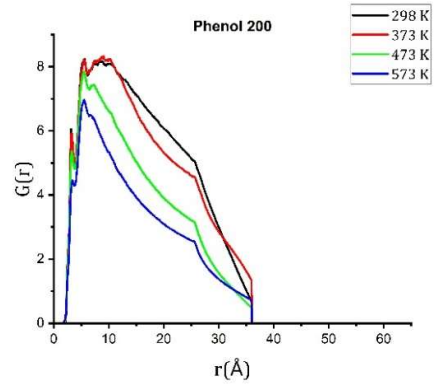

(b)

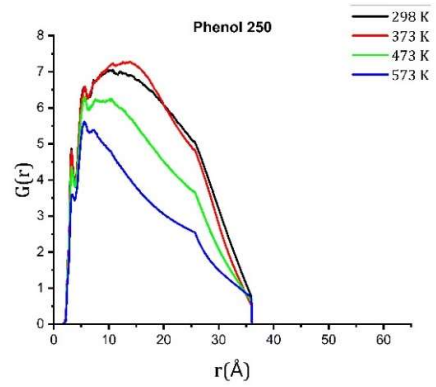

(c)

Fig. 5. Radial distribution functions for 150 (a), 200 (b), and 250 (c) phenol molecules adsorbed on API 5L X70 steel at 298K, 373K, 473K, and 573K.

Fig. 6 a, b and c, presents the radial distribution functions, g(r), for water molecules on API 5L X70 steel at loadings of 150, 200, and 250 molecules per simulation cell, over temperatures of 298K, 373K, 473K, and 573K. These data elucidate how thermal energy and molecular availability govern water's adsorption behavior. Across all concentrations, elevating the temperature from 298K to 573K causes a marked decrease in the height of the primary g(r) peak near the surface. This trend reflects enhanced desorption: increased kinetic energy overcomes the relatively weak van der Waals attraction between water and steel more readily than it disrupts the strong hydrogen bonds among water molecules, leading to rapid detachment from the interface.

When the temperature is held constant—particularly at 298 K, where adsorption is strongest—raising the number of water molecules from 150 to 250 significantly increases the first-peak intensity. This indicates a denser first adsorption layer as more molecules occupy available surface sites. Although the same concentration-driven enhancement persists at higher temperatures, its magnitude diminishes in line with the overall reduced adsorption.

These results demonstrate that water–steel interactions are highly temperature-sensitive, with adsorption collapsing at elevated temperatures, while at lower temperatures the extent of coverage is primarily dictated by molecule count. Together, thermal motion and concentration determine the density and ordering of water at the X70 steel surface, offering critical insight for predicting performance in moisture-laden, high-temperature environments.

3.1. Comparison of Adsorption Behavior for Phenol, Formaldehyde, and Water on X70 Steel

Interaction Analysis of the Phenol–Formaldehyde–Water Mixture on X70 Steel via Radial Distribution Functions: In Figure 7, the radial distribution functions, g(r), are shown for a ternary mixture of phenol, formaldehyde, and water in contact with the X70 steel surface under two simulation conditions. Here, N denotes the number of molecules of each component in the mixture:

(a) 150 molecules of each species (450 total) at 573K, At the elevated temperature of 573 K and with a relatively low total molecule count, the thermal energy of the adsorbates dominates. As a result, the first peak in g(r)—which corresponds to the local density in the primary adsorption layer near the steel surface—reflects primarily the strength of molecule–surface attractions rather than intermolecular forces. In this regime, phenol exhibits the highest first peak intensity, followed by formaldehyde and then water. This ordering indicates that, under high temperature conditions, phenol molecules have the strongest propensity to occupy the first adsorbed layer on X70 steel, with formaldehyde next and water last.

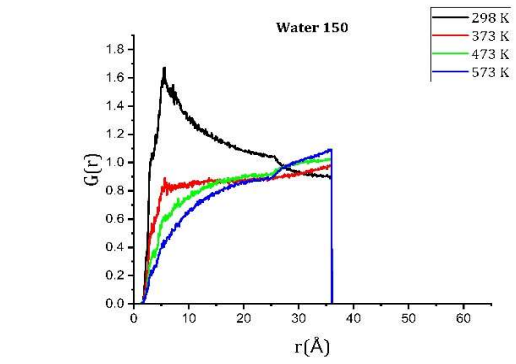

(a)

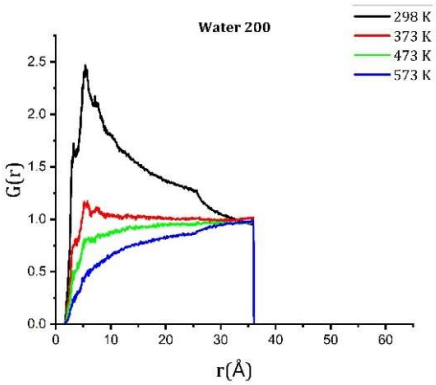

(b)

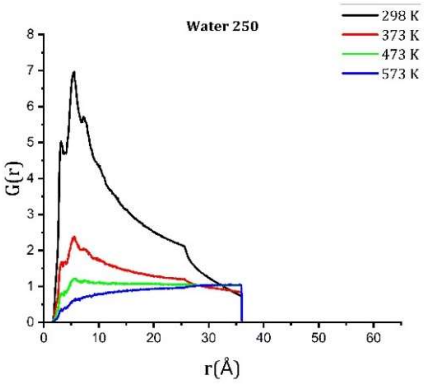

(c)

Fig. 6. Radial distribution functions for 150 (a), 200 (b), and 250 (c) water molecules adsorbed on API 5L X70 steel at 298K, 373K, 473K, and 573K.

(b) 250 molecules of each species (750 total) at 298K, At room temperature (298K) and a higher molecule concentration, intermolecular interactions (e.g., hydrogen bonds among phenol–water, formaldehyde–water, and phenol–formaldehyde pairs) play a larger role in defining both the overall structure and surface adsorption preferences. Under these conditions, formaldehyde shows the tallest first peak in g(r) compared to phenol and water. This finding reveals that, at 298K and with 250 molecules each, formaldehyde most readily accumulates in the first adsorption layer. Here, the balance between van der Waals adhesion of formaldehyde to the steel and its hydrogen-bonding network with neighboring molecules drives a higher local concentration of formaldehyde near the surface than of phenol or water.

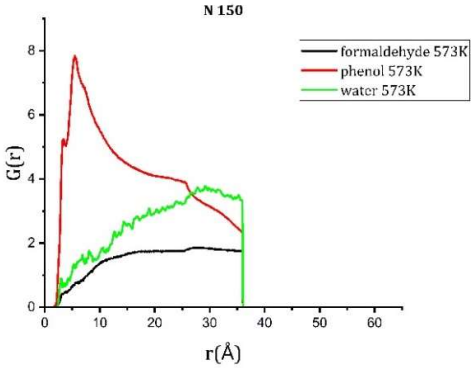

(a)

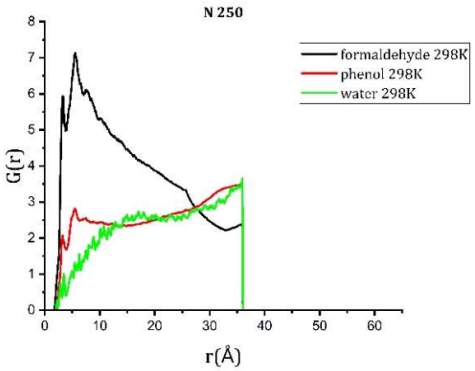

(b)

Fig. 7. Radial distribution functions for ternary mixtures of phenol, formaldehyde, and water adsorbed on the API 5L X70 steel surface: (a) 150 molecules of each component at 300 °C (573K) and (b) 250 molecules of each component at 25 °C (298K).

4. Conclusions

This study employs molecular dynamics simulations to investigate the effects of temperature and concentration on the interactions of phenol, formaldehyde, and water with API 5L X70 steel. A total of 38 distinct simulation cases spanning a wide range of operating conditions were performed. Analysis of the radial distribution functions (g(r)) between the adsorbates and the steel surface yielded the following principal findings:

1. With increasing temperature molecular kinetic energy, which systematically reduces the residence time of molecules near the surface and enhances desorption. In the RDFs, this manifests as a decrease in the height of the primary peak (corresponding to the first adsorption layer), indicating a lower

local density of adsorbates at higher temperatures.

2. Increasing the total number of adsorbate molecules—especially once the surface is fully covered—promotes the formation of multilayers. These additional layers alter both the local structure near the surface and the ordering in upper layers. In the RDF plots, these effects appear as changes in peak height, position, and notably peak broadening, underscoring the complexity of multilayer adsorption and the significant role of intermolecular forces alongside surface interactions.
3. Competitive Adsorption at High Temperature: For the ternary mixture at 573K with N = 150 molecules per component, direct molecule–surface interactions dominate the adsorption behavior. RDF analysis reveals that phenol exhibits the strongest affinity for the first adsorption layer, followed by formaldehyde and then water. This ordering reflects the relative strengths of these molecules' interactions with the steel surface under high temperature conditions.
4. At 298K with N = 250 molecules per component, competition for surface sites and strong intermolecular interactions (such as hydrogen bonds among phenol, formaldehyde, and water) govern adsorption preferences. Under these conditions, formaldehyde shows the highest tendency to occupy the first adsorption layer. This result indicates that, at ambient temperature and elevated concentration, the balance between formaldehyde's van der Waals adhesion to the steel and its hydrogen-bonding interactions with neighboring molecules favors its preferential adsorption over phenol and water.

These findings provide a predictive framework for understanding the corrosion susceptibility of X70 steel in environments relevant to composite-curing autoclaves, where high temperatures and the presence of phenol-formaldehyde reaction byproducts are unavoidable. Beyond their immediate implications, the results of this study may guide future research toward the development of more accurate computational models and the design of protective strategies for steels used in advanced composite manufacturing.

Funding Statement

This work was supported by the Imam Hossein University of Iran-Tehran.

Conflicts of Interest

The authors declare that there are no conflicts of interest.

Authors Contribution Statement

All authors contributed to the study conception and design. Material preparation, data collection and analysis were performed by Amir Hosein Bakhshandeh, Hadi Eivazi Bagheri., Seyyed Salman Seyyed Afghahi and Ali Asghar Ebrahimi Valmoozi. The first draft of the manuscript was written by Amir Hosein Bakhshandeh and Hadi Eivazi Bagheri, and all authors commented on previous versions. All authors read and approved the final manuscript.

References

[1] Gayakwad, N., Patil, V., Rao, B. M., Gokale, G. M., & Gurlhosur, K. (2021). Studies on *Rhoeo discolor* plant extract as a natural corrosion inhibitor. *Journal of Environmental Engineering and Science, 16*, 66–76. https://doi.org/10.1680/jenes.20.00008

[2] Satapathy, A. K., Gunasekaran, G., Sahoo, S. C., Amit, K., & Rodrigues, P. V. (2009). Corrosion inhibition by *Justicia gendarussa* plant extract in hydrochloric acid solution. *Corrosion Science, 51*(12), 2848–2856. https://doi.org/10.1016/j.corsci.2009.08.016

[3] Arora, P., Kumar, S., & Shukla, S. K. (2007). Inhibitive effect of Capparis decidua on corrosion of mild steel in acidic media. *E-Journal of Chemistry, 4*(4), 450–456. https://doi.org/10.1155/2007/852539

[4] Yıldız, R. (2015). An electrochemical and theoretical evaluation of 4,6-diamino-2-pyrimidinethiol as a corrosion inhibitor for mild steel in HCl solutions. *Corrosion Science, 90*, 544–553. https://doi.org/10.1016/j.corsci.2014.10.052

[5] Liu, H., Wang, L., & Liu, R. (2015). Experimental and theoretical studies on the corrosion inhibition of mild steel by triazole derivatives. *Journal of Molecular Liquids, 211*, 111–116. https://doi.org/10.1016/j.molliq.2015.06.040

[6] Kokalj, A. (2010). Is the analysis of molecular electronic structure of corrosion inhibitors sufficient to predict the trend of their inhibition performance? *Electrochimica Acta, 56*(2), 745–755. https://doi.org/10.1016/j.electacta.2010.09.065

[7] Obi-Egbedi, N. O., Obot, I. B., & El-Khaiary, M. I. (2011). Quantum chemical investigation and statistical analysis of the relationship between corrosion inhibition efficiency and molecular structure of xanthene and its derivatives on mild steel in sulphuric acid. *Journal of Molecular Structure, 1002*(1–3), 86–96. https://doi.org/10.1016/j.molstruc.2011.07.051

[8] Musa, A. Y., Kadhum, A. A. H., Mohamad, A. B., & Takriff, M. S. (2010). On the inhibition of mild steel corrosion by 4-amino-5-phenyl-4H-1,2,4-triazole-3-thiol. *Corrosion Science, 52*(2), 526–533. https://doi.org/10.1016/j.corsci.2009.09.040

[9] Ebenso, E. E., Arslan, T., Kandemirli, F., Love, I., Alemu, H., Umoren, S. A., & Obot, I. B. (2010). Quantum chemical investigations on quinoline derivatives as effective corrosion inhibitors for mild steel in acidic medium. *International Journal of Quantum Chemistry, 110*(14), 2614–2636. https://doi.org/10.1002/qua.22771

[10] Gece, G. (2008). The use of quantum chemical methods in corrosion inhibitor studies. *Corrosion Science, 50*(11), 2981–2992. https://doi.org/10.1016/j.corsci.2008.08.043

[11] Geerlings, P., De Proft, F., & Langenaeker, W. (2003). Conceptual density functional theory. *Chemical Reviews, 103*(5), 1793–1873. https://doi.org/10.1021/cr990029p

[12] Koopmans, T. (1934). Über die Zuordnung von Wellenfunktionen und Eigenwerten zu den einzelnen Elektronen eines Atoms. *Physica, 1*(1–6), 104–113. https://doi.org/10.1016/S0031-8914(34)90011-2

[13] Parr, R. G., Szentpály, L. v., & Liu, S. (1999). Electrophilicity index. *Journal of the American Chemical Society, 121*(9), 1922–1924. https://doi.org/10.1021/ja983494x

[14] Pearson, R. G. (1989). Absolute electronegativity and hardness: Application to inorganic chemistry. *Inorganic Chemistry, 27*(4), 734–740. https://doi.org/10.1021/ic00277a030

[15] Pearson, R. G. (1963). Hard and soft acids and bases. *Journal of the American Chemical Society, 85*(22), 3533–3539. https://doi.org/10.1021/ja00905a001

[16] Koopmans, T. (1934). Über die Zuordnung von Wellenfunktionen und Eigenwerten zu den einzelnen Elektronen eines Atoms. *Physica, 1*(1–6), 104–113. https://doi.org/10.1016/S0031-8914(34)90011-2

[17] Parr, R. G., & Yang, W. (1984). Density functional approach to the frontier-electron theory of chemical reactivity. *Journal of the American Chemical Society, 106*(14), 4049–4050. https://doi.org/10.1021/ja00326a036

[18] Thompson, A. P., Aktulga, H. M., Berger, R., Bolintineanu, D. S., Brown, W. M., Crozier, P. S., in 't Veld, P. J., Kohlmeyer, A., Moore, S. G., Nguyen, T. D., Shan, R., Stevens, M. J., Tranchida, J., Trott, C., & Plimpton, S. J. (2022). LAMMPS — A flexible simulation tool for particle-based materials modeling at the atomic, meso, and continuum scales. *Computer Physics Communications, 271*, 108171. https://doi.org/10.1016/j.cpc.2021.108171

.